ACS OMEGA

Open Access

http://pubs.acs.org/journal/acsodf

Article

Mechanical and Thermal Properties of Porous Nanocellulose/Polymer Composites: Influence of the Polymer Chemical Structure and Porosity

Naoki Tamura, Kota Hasunuma, Tsuguyuki Saito, and Shuji Fujisawa*

Cite This: *ACS Omega* 2024, 9, 19560−19565

Read Online

ACCESS | Metrics & More | Article Recommendations | Supporting Information

ABSTRACT: The excellent emulsifying capacity of nanocellulose allows for the preparation of porous nanocellulose/polymer composites through the emulsion templating process. However, the effects of the polymer chemical structure and porosity on the material properties have not been extensively explored. Here, we discuss the effects of these two factors on the thermal and mechanical properties of the composites. Two types of porous nanocellulose/polymer composites were fabricated with styrene-divinylbenzene (poly(St-*co*-DVB)) or styrene-poly(ethylene glycol) dimethacrylate (poly(St-*co*-EGDMA)) copolymers as the polymer phases. The porosity of the composite was changed up to ∼50% v/v by varying the aqueous phase volume fraction in the original nanocellulose-stabilized w/o emulsions. As the porosity increased, the thermal conductivity of the composite decreased. The mechanical properties were strongly influenced by the polymer type; the nanocellulose/poly(St-*co*-DVB) composite showed stiff but brittle behavior, whereas the nanocellulose/poly(St-*co*-EGDMA) composite showed higher strength and toughness. In both types of composites, the nanocelluloses served as reinforcing agents, contributing to the improvement of the mechanical properties.

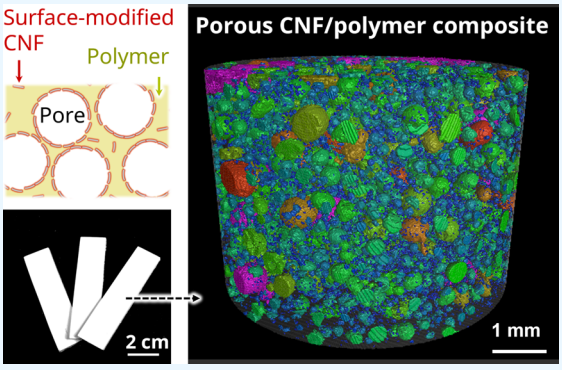

INTRODUCTION

Emulsion templating has attracted attention as a versatile method for fabricating porous polymeric materials;[1,2] the phase-separated structure of the emulsion enables the design of porous polymer architectures, thus offering the potential for applications such as absorbents, biomedical devices, membranes, lightweight foams, and tissue engineering scaffolds. Emulsions stabilized by solid fine particles, which are well-known as Pickering emulsions,[3−5] have shown great potential for the templating approach. Compared with molecular surfactants, the solid particles more stably adsorb at liquid/liquid interfaces,[6] which allows controlled syntheses of porous structures. Moreover, the solid particles have another advantage in that they do not plasticize the polymer matrices but rather reinforce the polymers.

Cellulose nanofibers (CNFs) are naturally occurring crystalline materials, and they satisfy the increasing demand for a sustainable and environmentally friendly stabilizer for Pickering emulsions.[7,8] The CNFs have high moduli and strengths[8,9] owing to their crystal structures and show unique rheological properties, such as high viscosity.[10,11] These mechanical and rheological properties of the CNFs play significant roles in the stabilization of emulsions against coalescence and creaming, making nanocellulose-stabilized emulsions highly attractive for use in foods, cosmetics, and pharmaceuticals. CNFs generally stabilize oil-in-water (o/w) emulsions by efficiently stabilizing the oil/water interfaces. The phase inversions of emulsions from o/w to water-in-oil (w/o) emulsions are facilitated by tuning the surface free energy of the CNFs via surface-selective chemical modification.[7,8]

Porous CNF/polymer composite materials can be fabricated by templating emulsions with the stable structures of o/w[12] or w/o[13,14] emulsions. The CNFs act as emulsifiers and also serve as reinforcing agents in the final composites owing to their excellent mechanical properties. The porous structures can be tailored by controlling the structures of the original emulsions to enable tuning of the mechanical properties.[14] Although the material properties of porous composites have been reported thus far, the influence of the chemical structure of the polymer phase on the mechanical properties of porous CNF/polymer composites has yet to be explored.

Here, we investigate the effects of the chemical structures of the CNF/polymer composites on their thermal conductivities

Received: February 6, 2024
Revised: April 3, 2024
Accepted: April 4, 2024
Published: April 15, 2024

Scheme 1. Emulsion-Templating Approach for the Preparation of Porous CNF/Polymer Composite Materials[a]

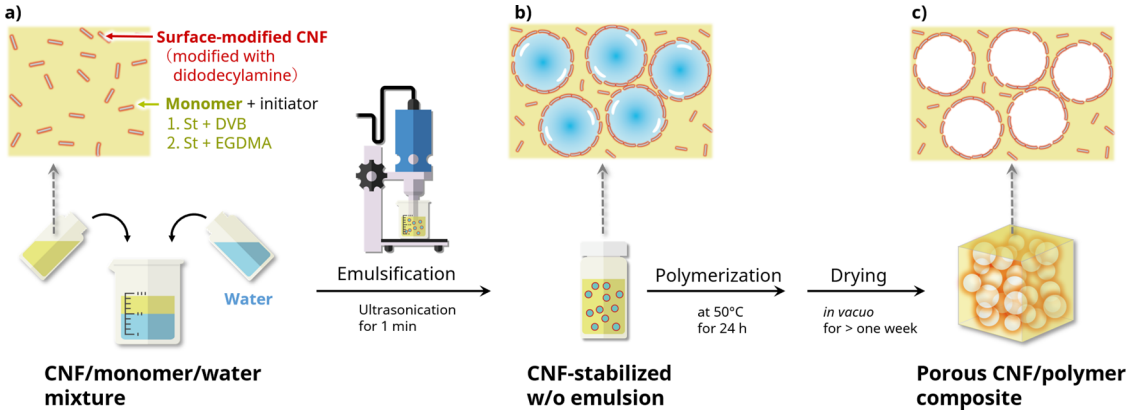

[a]Schematic illustrations of (a) the CNF/monomer/water mixture, where the concentration of the surface-modified CNF was 0.8% w/w (0.5% w/w of CNF and 0.3% w/w of didodecylamine); the surface carboxylate groups of the CNFs, which were introduced by TEMPO-mediated oxidation, were modified via ionic bonding with didodecylamine; (b) CNF-stabilized w/o emulsion; and (c) porous CNF/polymer composite material.

and mechanical properties. Porous CNF/polymer composites were fabricated by templating with the structures of w/o emulsions stabilized by CNFs derived from wood (Scheme 1). To alter the chemical structure of the polymer phase, two cross-linking agents, divinylbenzene (DVB) or polyethylene glycol dimethacrylate (EGDMA), were used for the polymerization of styrene monomers. Furthermore, the porosities of the composites were varied by adjusting the volume fractions of the aqueous phases in the original w/o emulsions.

EXPERIMENTAL SECTION

Materials. TEMPO-oxidized pulp with a carboxy content of ~1.78 mmol g^{-1} was kindly provided by DKS Co. Ltd. Styrene (St), DVB, 2,2′-azobis(2,4-dimethylvaleronitrile) (ADVN), didodecylamine, sorbitan oleate and other chemicals were obtained from Wako Chemical Co., Ltd. (Japan) and used as received. EGDMA (n = approximately 4) was purchased from TCI Chemicals (Japan) and used as received. The oxidized pulp was suspended in distilled water at 0.5% (w/w) and passed twice through high-pressure wet milling equipment (HJP-25005X, Sugino Machine Limited, Japan) at 150 MPa to mechanically disintegrate the oxidized pulp into CNFs. The CNF aqueous dispersion was filtered through a 20 μm mesh to remove the nonfibrillated parts.

Preparation of CNF-Stabilized w/o Emulsions. The surfaces of the CNFs were modified with didodecylamine by forming ionic bonds with the carboxy groups of the CNFs, as previously reported.[15] Most of the surface carboxy groups of CNFs were modified with didodecylamine (Figure S1). The surface-modified CNFs were solvent-exchanged with a mixture of St/DVB (1:1 in volume) containing ADVN, where the concentration of the CNFs was adjusted to 0.5% w/w. Water was added to the system to achieve water volume fractions of 10, 30, and 50%. Then, $2C_{12}$−CNF-stabilized w/o emulsions with different volume fractions of the water phases were prepared by sonicating the mixtures in a water bath for 1 min. $2C_{12}$−CNF-stabilized w/o emulsions with different monomer mixtures (St and EGDMA) were also prepared with the same procedure. In this study, DVB and EGDMA were used as cross-linking agents because the St monomer alone was not able to maintain the structures of the original emulsions.

Preparation of Porous CNF/Polymer Composite. Two types of $2C_{12}$−CNF-stabilized w/o emulsions were placed in molds and degassed at room temperature for 1 h with a vacuum pump. Then, the mold was placed in an oven at 50 °C for 24 h to polymerize the monomers in the oil phases, and porous CNF/poly(St-*co*-DVB) and CNF/poly(St-*co*-EGDMA) composites were obtained.

Analyses. Field-emission scanning electron microscopy (SEM) (S-4800, Hitachi, Japan) was performed at 1 kV. The samples were coated with osmium by an osmium coater (Neo-Osmium Coater, Meiwafosis, Japan) at 5 mA for 10 s. Morphological analyses of the porous composites were carried out with a microfocus X-ray CT system (InspeXio SMX-100CT, Shimadzu Corporation, Japan). Fourier transform infrared (FT-IR) analyses of the CNF films were carried out with an FT-IR spectrometer (FT/IR-6100, JASCO, Japan) under transmission mode from 400 to 4000 cm^{-1} with a 4 cm^{-1} resolution. Bulk density measurements were performed to determine the porosities of the composites. The porosity was calculated with the following equation:

$$\text{Porosity} = \left(1 - \frac{\rho_b}{\rho_t}\right) \times 100 \quad (1)$$

where ρ_b is the bulk density (g cm^{-3}) measured with a powder pycnometer (Geopyc1365, Micromeritics, USA) and ρ_t is the true density (g cm^{-3}); the true density of the composite was determined experimentally with bulk density measurements of the CNF/polymer mixture. A three-point bending test was performed with a mechanical testing machine (EZ-SX, Shimadzu Corp., Japan) equipped with a 500 N load cell. The dimensions of the specimens, spans, and crosshead speeds were set to 15 × 60 × 2 mm^3, 40 mm, and 1 mm min^{-1}, respectively. The thermal conductivities of the porous CNF/polymer composites were measured with a thermal constant analyzer (TPS2500S, Hot Disk Inc., Sweden), and cylindrical specimens with diameters and thicknesses of 12 and 4 mm, respectively, were used.

RESULTS AND DISCUSSION

Composite Structure. Figure 1 shows images of the composites. CNF/poly(St-*co*-DVB) and CNF/poly(St-*co*-EGDMA) composites were prepared by templating with CNF-stabilized w/o emulsions (Scheme 1). Regardless of the type of monomer or the aqueous phase volume fractions in the

https://doi.org/10.1021/acsomega.4c01206
ACS Omega 2024, 9, 19560−19565

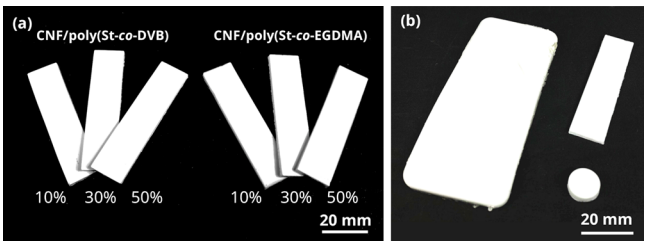

Figure 1. (a) Images of the porous CNF/poly(St-*co*-DVB) and CNF/poly(St-*co*-EGDMA) composites with different porosities, where the values listed are the volume fractions of the aqueous phase in the original w/o emulsions. (b) CNF/poly(St-*co*-EGDMA) composites molded in different shapes.

original w/o emulsions (ranging from 10 to 50% (v/v)), it was possible to prepare uniform composite materials in every case. Various material shapes were designed (Figure 1b) since the original emulsions were flowable and could be cast into molds of any size and shape.

Porous structures were constructed with both the CNF/poly(St-*co*-DVB) and CNF/poly(St-*co*-EGDMA) composite systems (Figure 2). The pores were distributed homogeneously throughout the samples (Figures 2a–f and S2) because the viscosities of the original w/o emulsions were high due to the presence of CNFs modified with didodecylamine, which enabled stabilization of the emulsions against sedimentation or creaming of the water droplets during the polymerization process. A thin and uniform CNF layer was observed at the polymer–air interface (Figure 2h), demonstrating that the CNF had efficiently stabilized the original w/o emulsion system by attaching it to the monomer–water interface. When the CNFs without the surface modification were used in the composite preparation process, the CNF/monomer/water system was not able to form a w/o emulsion but resulted in an o/w emulsion for both the St/DVB and St/EGDMA monomer systems (Figure S3); powder CNF shelled polymer microparticles were obtained after polymerization, as reported in previous studies.[16,17] Therefore, it was necessary to chemically tailor the CNF surfaces to form the porous composites described here.

The porosities of the composites increased with increasing volume fractions of the aqueous phase in the original w/o emulsions, showing comparable values irrespective of the monomer type (Figure 3 and Table S1). This suggests that the

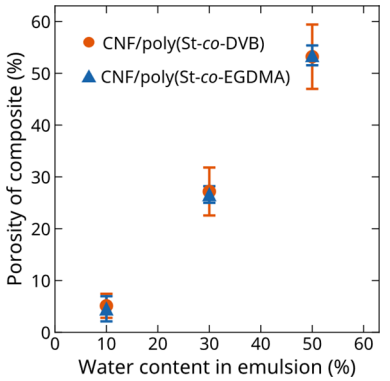

Figure 3. Porosities of CNF/poly(St-*co*-DVB) and CNF/poly(St-*co*-EGDMA) composites as a function of the water contents in the original w/o emulsions (% v/v).

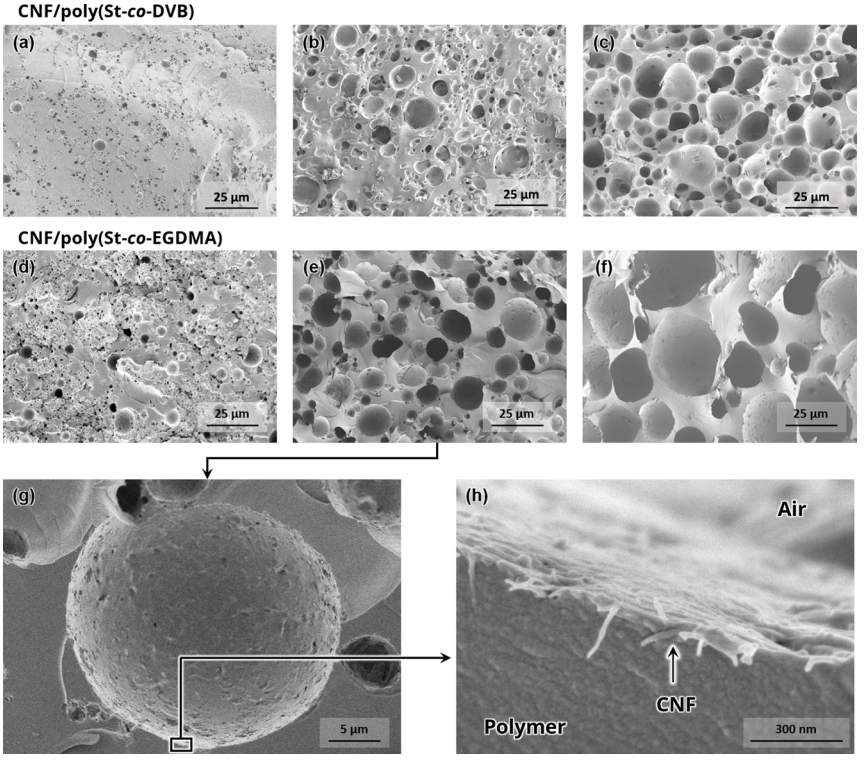

Figure 2. Cross-sectional SEM images of the porous CNF/poly(St-*co*-DVB) and CNF/poly(St-*co*-EGDMA) composites, where the volume fractions of the aqueous phase in the original w/o emulsions were (a, d) 10, (b, e) 30, and (c, f) 50% v/v. (g, f) Magnified images of the solid–air interface.

https://doi.org/10.1021/acsomega.4c01206
ACS Omega 2024, 9, 19560–19565

CNFs effectively stabilized the emulsions during the polymerization. However, it was observed that a lower water phase ratio in the emulsion tends to result in a decreased porosity of the resulting composite materials. This is likely because the impact of volume shrinkage becomes more pronounced in samples with a higher polymer ratio.

As shown in the SEM images (Figure 2), the pores in the composites appeared to be closed-cell structures, even with a porosity of ∼50% v/v. A "closed-cell" structure is commonly used to describe a formation without interconnected pores. However, the pores are not truly closed because the water molecules were removed from the composite. Therefore, it is likely that the composite had quasiclosed-cell structures, as often observed in Pickering emulsion-templated porous materials.[1]

The sizes of the pores in the composites became larger with increasing volume fractions of the aqueous phases in the original w/o emulsions (Figure 2). This is likely because the coalescence of the water droplets occurred due to collisions during the polymerization process. Although we tried to increase the porosity of the composite by raising the water volume fractions in the original w/o emulsions to 70% v/v or higher, the emulsions were converted to o/w emulsions and did not provide the porous composites obtained above (Figure S3). Kralchevsky et al. used a thermodynamic model and provided a theoretical discussion of phase inversion for particle-stabilized emulsions, showing that an aqueous phase volume fraction of 50% v/v was the threshold for catastrophic phase inversion.[18] This was experimentally verified by Binks and Lumsden with hydrophobic silica-stabilized w/o emulsions that were catastrophically converted, without hysteresis, to o/w emulsions at aqueous phase volume fractions of ∼70% v/v.[19] Therefore, phase inversions likely occurred in this study at large volume fractions of the aqueous phase. Previous studies reported that nanoparticles such as surface-functionalized titania[20] and silica[21] were capable of solely stabilizing high internal phase Pickering w/o emulsions (HIPEs) with internal aqueous phase volumes exceeding 70%. In the Pickering-HIPEs approach, the crucial factor for stabilizing the interfaces in w/o emulsions was control of the nanoparticle surface wettability. Therefore, in order to increase the aqueous phase volume fraction, optimizing the surface functional groups of the CNFs is nescessary in future work.

Thermal Properties. Figure 4 shows the thermal conductivities of the composites. The conductivity of the composites decreased with increasing porosity. The mixture law provides a simple but useful review of the thermal conductivities of porous solids:[22]

$$\lambda_{tot} = (1 - \rho)\lambda_{sol} + \rho\lambda_{air} \quad (2)$$

where λ_{sol} is that of the composite material at 0% porosity, λ_{air} is the thermal conductivity of the air, λ_{air} is the thermal conductivity of air at 20 °C (0.026 W m^{-1} K^{-1}),[23] and ρ is the porosity of the composite. The thermal conductivities of the polymer phases, which were experimentally determined with a thermal constant analyzer, were 0.223 and 0.219 W m^{-1} K^{-1} for the CNF/poly(St-*co*-DVB) and CNF/poly(St-*co*-EGDMA) composites, respectively. Consequently, the expected lines for the CNF/poly(St-*co*-DVB) and CNF/poly(St-*co*-EGDMA) composites were λ = 0.219 (1 − ρ) + 0.026 and λ = 0.223 (1 − ρ) + 0.026, respectively. In this work, the contribution of radiative thermal conductivity was considered small because the densities of our materials were as high as > ∼50% v/v, and moreover, the temperature increases of the samples during the measurements were less than 1 K. Therefore, the porosity was the dominant factor in determining the thermal conductivity in this case. When the expected lines were compared with the experimental values in Figure 4, it was observed that as porosity increased, the experimental values tended to be higher than those predicted by the line. From Equation 2, one reason for this could be that an increase in λ_{sol} led to an increase in the value of λ_{sol}. As observed in the SEM images in Figure 2, CNFs are oriented and accumulated at the interface. Such accumulated CNFs have been reported to exhibit excellent thermal conductivity.[24,25] Therefore, when the porosity of the composite is increased, the surface area of this interface increases, which is thought to result in a higher thermal conductivity in λ_{sol}. The thermal conductivity of the 50% CNF/poly(St-*co*-DVB) and CNF/poly(St-*co*-EGDMA) composites is 0.10 and 0.13 W m^{-1} K^{-1}, respectively. However, these values are still higher than those of typical insulating materials. According to a linear approximation shown in Figure 4, increasing the porosity of the CNF/poly(St-*co*-EGDMA) composite to approximately 90% could reduce its thermal conductivity to ∼0.04 W m^{-1} K^{-1}, which is comparable to that of commercial polystyrene foam.[26] Therefore, an increase in the porosity is necessary for further improvement of the insulation properties.

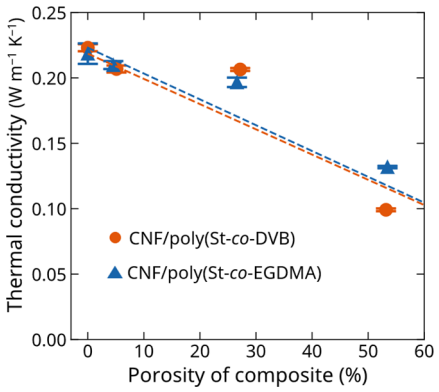

Figure 4. Thermal conductivities of porous CNF/poly(St-*co*-DVB) and CNF/poly(St-*co*-EGDMA) composites as functions of the porosities (% v/v). The dotted lines are the fitting results for the experimentally obtained thermal conductivities (λ) of the composites. Orange line: CNF/poly(St-*co*-DVB), λ = 0.219 (1 − ρ) + 0.26. Blue line: CNF/poly(St-*co*-EGDMA), λ = 0.223 (1 − ρ) + 0.26.

Mechanical Properties. Figure 5 shows the mechanical properties of the porous CNF/polymer composites obtained by three-point bending tests. The CNF/poly(St-*co*-DVB) composite exhibited a higher modulus but lower strength and strain at failure than the CNF/poly(St-*co*-EGDMA) composite. Since both composites had the same CNF contents and comparable porous structures, this was due to the mechanical properties of each copolymer. The CNF/poly(St-*co*-EGDMA) composite showed excellent toughness (2.8 MJ m^{-3}) that was approximately 10 times higher than that of CNF/poly(St-*co*-DVB) (0.27 MJ m^{-3}) with porosities of approximately 10% (Figure 5a); EGDMA, which is a longer and more flexible cross-linking agent than DVB, enhanced the toughness of the composite.[27] The bending modulus and strength of the composites decreased as the porosity increased. Dupont et al. used HIPEs with cellulose nanocrystals modified with a hydrophobic function (CNC-Br) to prepare CNF-Br/

https://doi.org/10.1021/acsomega.4c01206
ACS Omega 2024, 9, 19560−19565

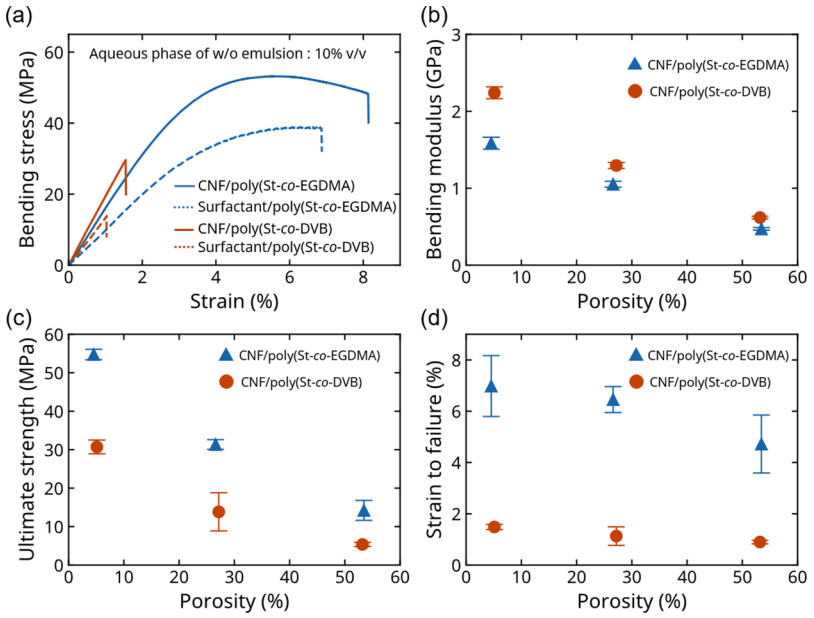

Figure 5. (a) Bending stress−strain curves. The porous materials were prepared from w/o emulsions stabilized by surface-modified CNFs or a surfactant (sorbitan oleate). The volume fractions of the aqueous phase in the original w/o emulsions were set to 10% v/v. (b) Bending modulus, (c) ultimate strength, and (d) strain to failure for porous CNF/poly(St-*co*-DVB) and CNF/poly(St-*co*-EGDMA) composites as a function of porosity (% v/v).

poly(St-*co*-DVB) composites with porosities between 75 and 85%,[14] where the compressive modulus was in the range of 1.5−2.1 MPa. They reported that the compressive modulus tended to decrease with increasing porosity, and this was concluded to be due to the effect of the fraction of the continuous phase rather than cell size, as predicted by the Gibson and Ashby model.[28] A similar observation can be made in our system, suggesting that the modulus and strength changed based on the fraction of the phase consisting of CNF and polymer. The relationship between the cell size and material properties in our system is currently under detailed investigation. Importantly, when a surfactant (sorbitan oleate) was used as the emulsifier instead of the surface-modified CNFs, the porous surfactant/polymer composite showed a lower modulus, strength, and strain at failure for each composite (Figure 5a). Therefore, CNFs acted as reinforcement agents and improved the mechanical properties of the composites.

CONCLUSIONS

In conclusion, we investigated the mechanical and thermal properties of porous CNF/polymer composite materials by varying the chemical structure and porosity of the polymer. Two types of composites, CNF/poly(St-*co*-DVB) and CNF/poly(St-*co*-EGDMA) were fabricated via the emulsion-templating process. The porosities of the composites were adjusted up to ∼50% v/v by altering the aqueous phase volume fractions in the original w/o emulsions, and increases in the volume fractions of the aqueous phases resulted in increased porosities and pore sizes in the composites. Despite attempts to increase the composite's volume fraction to 70% or higher, it was found that the w/o emulsions became unstable under the experimental conditions, making it impossible to prepare porous composites. These composites exhibited robust structures with homogeneous pore distributions throughout. The thermal properties varied with the porosity but were independent of the polymer's chemical structure. A higher porosity for a composite led to a decrease in thermal conductivity. In contrast, the mechanical properties of the composites varied with the type of polymer phase; the CNF/poly(St-*co*-DVB) composite had a slightly lower modulus but much higher strength and toughness than the CNF/poly(St-*co*-EGDMA) composite. In the composites, the CNFs served as reinforcing agents, contributing to the improvement of the mechanical properties. The scalability and ease of designing the molded structures with this material are attractive for various applications, such as lightweight structural components, insulation materials, and specialized biomedical devices where tailored mechanical and thermal properties are crucial.

ASSOCIATED CONTENT

Supporting Information

The Supporting Information is available free of charge at https://pubs.acs.org/doi/10.1021/acsomega.4c01206.

FT-IR spectra of CNF, X-ray CT analysis, and SEM images of composites (PDF)

AUTHOR INFORMATION

Corresponding Author

Shuji Fujisawa − *Department of Biomaterial Sciences, Graduate School of Agricultural and Life Sciences, The University of Tokyo, Tokyo 113-8657, Japan;* orcid.org/0000-0002-5221-6781; Email: afujisawa@g.ecc.u-tokyo.ac.jp

Authors

Naoki Tamura − *Department of Biomaterial Sciences, Graduate School of Agricultural and Life Sciences, The University of Tokyo, Tokyo 113-8657, Japan*

Kota Hasunuma − *Department of Biomaterial Sciences, Graduate School of Agricultural and Life Sciences, The University of Tokyo, Tokyo 113-8657, Japan*

Tsuguyuki Saito − *Department of Biomaterial Sciences, Graduate School of Agricultural and Life Sciences, The University of Tokyo, Tokyo 113-8657, Japan;* orcid.org/0000-0003-1073-6663

Complete contact information is available at: https://pubs.acs.org/10.1021/acsomega.4c01206

Author Contributions

S.F. conceived the project. N.T. and K.F. prepared the samples and performed all of the analysis. All authors discussed the data and wrote the manuscript.

Notes

The authors declare no competing financial interest.

■ ACKNOWLEDGMENTS

This research was supported by Grants-in-Aid for Scientific Research (Grant Nos. JP23H02270 to S.F., JP21H04733 to T.S.) from the Japan Society for the Promotion of Science (JSPS), and JST CREST Grant No. JPMJCR22L3 (to T.S. and S.F.) from Japan Science and Technology Agency (JST).

■ REFERENCES

(1) Zhang, T.; Sanguramath, R. A.; Israel, S.; Silverstein, S. M. Emulsion Templating: Porous Polymers and Beyond. *Macromolecules* **2019**, *52*, 5445−5479.
(2) Elsevier Ltd September 22 Silverstein, M. S. Emulsion-templated polymers: Contemporary contemplations. *Polymer.* **2017**, *126*, 261−282.
(3) Ramsden, W. Separation of solids in the surface-layers of solutions and 'suspensions' (observations on surface-membranes, bubbles, emulsions, and mechanical coagulation).—Preliminary account. *Proc. R. Soc. London* **1904**, *72*, 156−164.
(4) Pickering, S. U. CXCVI.—Emulsions. *Journal of the Chemical Society, Transactions* **1907**, *91*, 2001−2021.
(5) Binks, B. P. Particles as surfactants—similarities and differences. *Curr. Opin. Colloid Interface Sci.* **2002**, *7*, 21−41.
(6) Levine, S.; Bowen, B. D.; Partridge, S. J. Stabilization of emulsions by fine particles I. Partitioning of particles between continuous phase and oil/water interface. *Colloids Surf.* **1989**, *38*, 325−343.
(7) Fujisawa, S.; Togawa, E.; Kuroda, K. Nanocellulose-stabilized Pickering emulsions and their applications. *Sci. Technol. Adv. Mater.* **2017**, *18*, 959−971.
(8) Elsevier Ltd December 1 Zhu, M.; Huan, S.; Liu, S.; Li, Z.; He, M.; Yang, G.; Liu, S.; McClements, D. J.; Rojas, O. J.; Bai, L. Recent development in food emulsion stabilized by plant-based cellulose nanoparticles. *Curr. Opin. Colloid Interface Sci.* **2021**, *56*, No. 101512.
(9) Miao, C.; Tayebi, M.; Hamad, W. Y. Investigation of the formation mechanisms in high internal phase Pickering emulsions stabilized by cellulose nanocrystals. *Philosophical Transactions of the Royal Society A: Mathematical, Physical and Engineering Sciences* **2018**, *376*, No. 20170039.
(10) Tanaka, R. Rheological Properties of Nanocellulose Dispersions in the Dilute Region: Current Understanding and Future Perspectives. *Nihon Reoroji Gakkaishi* **2022**, *50*, 73−82.
(11) Elsevier B.V. January 1 Xu, Y.; Atrens, A.; Stokes, J. R. A review of nanocrystalline cellulose suspensions: Rheology, liquid crystal ordering and colloidal phase behaviour. *Adv. Colloid Interface Sci.* **2020**, *275*, No. 102076.
(12) Qiao, M.; Yang, X.; Zhu, Y.; Guerin, G.; Zhang, S. Ultralight Aerogels with Hierarchical Porous Structures Prepared from Cellulose Nanocrystal Stabilized Pickering High Internal Phase Emulsions. *Langmuir* **2020**, *36*, 6421−6428.
(13) Blaker, J. J.; Lee, K. Y.; Li, X.; Menner, A.; Bismarck, A. Renewable nanocomposite polymer foams synthesized from Pickering emulsion templates. *Green Chem.* **2009**, *11*, 1321−1326.
(14) Dupont, H.; Fouché, C.; Dourges, M. A.; Schmitt, V.; Héroguez, V. Polymerization of cellulose nanocrystals-based Pickering HIPE towards green porous materials. *Carbohydr. Polym.* **2020**, *243*, No. 116411.
(15) Fujisawa, S.; Saito, T.; Isogai, A. Nano-dispersion of TEMPO-oxidized cellulose/aliphatic amine salts in isopropyl alcohol. *Cellulose* **2012**, *19*, 459−466.
(16) Fujisawa, S.; Togawa, E.; Kuroda, K.; Saito, T.; Isogai, A. Fabrication of ultrathin nanocellulose shells on tough microparticles: Via an emulsion-templated colloidal assembly: Towards versatile carrier materials. *Nanoscale* **2019**, *11*, 15004−15009.
(17) Fujisawa, S.; Kaku, Y.; Kimura, S.; Saito, T. Magnetically Collectable Nanocellulose-Coated Polymer Microparticles by Emulsion Templating. *Langmuir* **2020**, *36*, 9235−9240.
(18) Kralchevsky, P. A.; Ivanov, I. B.; Ananthapadmanabhan, K. P.; Lips, A. On the Thermodynamics of Particle-Stabilized Emulsions: Curvature Effects and Catastrophic Phase Inversion. *Langmuir* **2005**, *21*, 50−63.
(19) Binks, B. P.; Lumsdon, S. O. Catastrophic Phase Inversion of Water-in-Oil Emulsions Stabilized by Hydrophobic Silica. *Langmuir* **2000**, *16*, 2539−2547.
(20) Menner, A.; Ikem, V.; Salgueiro, M.; Shaffer, M. S. P.; Bismarck, A. High internal phase emulsion templates solely stabilised by functionalised titania nanoparticles. *Chem. Commun.* **2007**, No. 41, 4274−4276.
(21) Ikem, V. O.; Menner, A.; Bismarck, A. High Internal Phase Emulsions Stabilized Solely by Functionalized Silica Particles. *Angew. Chem., Int. Ed.* **2008**, *47*, 8277−8279.
(22) Collishaw, P. G.; Evans, J. R. G. An assessment of expressions for the apparent thermal conductivity of cellular materials. *J. Mater. Sci.* **1994**, *29*, 2261−2273.
(23) Reid, R. C.; Sherwood, T. K. *The Properties of Gases and Liquids: Their Estimation and Correlation*, 2nd ed.; McGraw-Hill: New York, 1966.
(24) Smalyukh, I. I. Thermal Management by Engineering the Alignment of Nanocellulose. *Adv. Mater.* **2021**, *33*, No. 2001228.
(25) Uetani, K.; Hatori, K. Thermal conductivity analysis and applications of nanocellulose materials. *Sci. Technol. Adv. Mater.* **2017**, *18*, 877−892.
(26) Ashby, M. F.; Shercliff, H.; Cebon, D. *Materials: Engineering, Science, Processing and Design*, 2nd ed.; Butterworth-Heinemann, 2010.
(27) Livshin, S.; Silverstein, M. S. Cross-linker flexibility in porous crystalline polymers synthesized from long side-chain monomers through emulsion templating. *Soft Matter* **2008**, *4*, 1630−1638.
(28) Gibson, L. J.; Ashby, M. F.; Wolcott, M. P. *Cellular Solids: Structure and Properties*, 2nd ed.; Cambridge University Press, 1990.